Volume 3, Issue 12, December 2013 ISSN: 2277 128X
International Journal of Advanced Research in Computer Science and Software Engineering
Research Paper
Available online at: www.ijarcsse.com

Polarization Shearing Interferometer (PSI) Based Wavefront Sensor for Adaptive Optics

M.Mohamed Ismail[1], M.Mohamed Sathik[2]
Research Department of Computer Science,
Sadakathullah Appa College (Autonomous),
Tirunelveli -11, Tamilnadu, India

Abstract - A Polarization Shearing Interferometer (PSI) based wavefront sensor for Adaptive Optics applications has been reported. It is simple and easily adoptable in any adaptive optical set up. In this method, a single interferometric record, where both the x-shear and y-shear have been combined, is able to provide complete information of the wave front using Fourier transform techniques. The efficacy of this method for Adaptive Optics application is discussed.

Keywords: Adaptive Optics, Babinet Compensator, Zernike Polynomials, Shearing Interferometry

I. INTRODUCTION

In many astronomical and defence Optical/IR imaging application, to compensate the effects due to atmospherical turbulence in the path of the incoming beam a close loop optical system known as Adaptive Optics (AO) is presently a common requirement. The most critical component in the Adaptive Optics system is the wavefront sensor. The three methods of wavefront sensing that have been generally used are 1) Shack Hartmann sensor 2) Curvature Sensor and 3) Shearing Interferometry. Way back in 1987, Hardy and Mac Govern[1] had given an overview of the lateral shearing interferometry and its potential for various wavefront sensing applications. Lateral shearing interferometry was employed as the wavefront sensor in one of the earliest system for real time atmospheric corrections (Hardy, et.al[2] and Hardy[3]). These lateral shearing interferometers use crossed double frequency gratings. Humphries[4] et.al. used a Jamie's Interferometer to produce lateral shear for the purpose. One of the major drawback of these interferometric techniques is the requirement of orthogonal pair of interferograms for wavefront reconstruction. Some methods suggest using two detectors simultaneously while others suggest recording sequentially using the same detector. Although conventional methods like Shack-Hartmann and curvature sensing are often used in the present day wavefront sensing devices, shearing interferometer offers better choice for its linearity, better signal processing and added spatial information. For these advantages a simple lateral shearing interferometer using Babinet compensators (BC) was described by Saxena[5,6]. The technique was further improved employing two crossed BCs[7]. A detailed theory on the use of this PSI device as a wavefront sensor for Adaptive Optics applications was provided by Saxena et al.[8,9]

II. THEORY OF THE PSI BASED SENSOR

The Fourier theory for the two crossed Babinet compensator has been reported [9]. The theory is further extended to retrieve the wavefront slope using Fourier transform methods from the intensity data. The wavefront is reconstructed using the derivatives of the Zernike polynomials expressed as a linear combination of Zernike polynomials[10] and suitable phase unwrapping technique.

The Zernike polynomials can be written as

$$\begin{aligned} Z_{i\,even} &= \sqrt{n+1}R_n^m(\rho)\sqrt{2}\cos(m\theta), \quad for \ \ m \neq 0 \\ Z_{i\,odd} &= \sqrt{n+1}R_n^m(\rho)\sqrt{2}\sin(m\theta), \quad for \ \ m \neq 0 \\ Z_i &= \sqrt{n+1}R_n^0(\rho), \qquad\qquad for \ \ m=0 \end{aligned} \tag{1}$$

$$R_n^m(\rho) = \sum_{s=0}^{\frac{n-m}{2}} \frac{(-1)^s (n-s)!}{s!\left(\frac{n+m}{2}-s\right)!\left(\frac{n-m}{2}-s\right)!}\rho^{n-2s}$$

where

The values of n and m are always integral and satisfy m $\leq$ n, n-|m| = even. The index i is a mode ordering number and is a function of n and m.

The partial derivatives of W(x,y) are obtained as

$$\frac{\partial W}{\partial x} = \sum_{i=0}^{N} C_i \frac{\partial Z_i}{\partial x}$$

$$\frac{\partial W}{\partial y} = \sum_{i=0}^{N} C_i \frac{\partial Z_i}{\partial y} \quad (2)$$

As discussed earlier the derivatives of the Zernike polynomials can be expressed as linear combination of Zernike polynomial, substituting

$$\frac{\partial Z_n}{\partial x} = \sum_{i=2}^{N} \varepsilon_{nm} Z_n$$

Therefore

$$\frac{\partial Z_n}{\partial y} = \sum_{i=2}^{N} \gamma_{nm} Z_n \quad (3)$$

where ε_{mn} and γ_{mn} are the constants of the matrix as given by Noll (1970)
The matrix equation describing the wavefront gradients to the Zernike polynomial can be written as

$$\frac{\partial W}{\partial x} = \sum_{i=2}^{N} C_n \varepsilon_{nm} Z_n$$

$$\frac{\partial W}{\partial y} = \sum_{i=2}^{N} C_n \gamma_{nm} Z_n \quad (4)$$

where C_n are the Zernike Coefficients.
The intensity at the detector plane is given by

$$I(x, y) = \left[k_o + k_1 \cos \frac{2\pi}{\lambda} \Delta W(x, y) \right] \quad (5)$$

Where $k_o = a_o^2 + b_o^2$, $k_1 = 2a_o b_o$, $\Delta w(x, y) = w\left(x + \frac{s}{2}, y + \frac{t}{2} \right) - w\left(x - \frac{s}{2}, y - \frac{t}{2} \right)$ and S & T are the shears in the x nd y directions respectively.
For values of shear < 0.1 of the pupil, the overlap region is close to the original pupil. In such case, $\Delta W(x,y)$ can be written as

$$\Delta W(x, y) = \frac{\partial w}{\partial x} S + \frac{\partial w}{\partial y} T \quad (6)$$

The value of shear is determined from the equation

$$Shear = 2R (n_e - n_o) \tan\theta \quad (7)$$

The fringe frequency defines the number of fringes contained in the interferogram. Sensitivity of any shearing interferometer depends up on the shear value. The larger the shear value the better is the sensitivity. The appropriate value of the shear is chosen based on the pupil aperture, fringe parameters, detector resolution and the dynamic range. . shear S_r is given by

$$S_r = (S^2 + T^2)^{1/2} \quad (8)$$

where S and T are the shears in the x and y directions respectively.

Fig.1. Simulated Interferogram

III. Basis of determining X & Y Slope from a Single PSI Record

Consider equation (4) describing the wavefront gradients to the Zernike polynomial where the C_n are the Zernike Coefficients. In the x derivative, the Zernike Coefficient Cn corresponding to the tilt about x axis is undetermined. To determine the coefficient C_n corresponding to x – tilt, it becomes mandatory to differentiate with respect to y. Therefore the final interferogram corresponding to the incoming wavefront is given by equation (5). In the theory explained above, the emerging beam from the analyzer correspond to

$$\Delta W(x,y) = \frac{\partial w}{\partial x} S + \frac{\partial w}{\partial y} T \qquad (9)$$

where both the derivatives are combined in the single interferometric record and all the coefficients are accounted for in the process and determined using the least squares methods. Thus, by this method it is possible to retrieve all the information from single interferometric record so obtained.

IV. PHASE ESTIMATION

The fringe pattern of the interferogram can be redefined as

$$I(x,y) = a(x,y) + b(x,y)\cos\{2\pi f_o.r - \phi(r)\} \qquad (10)$$

Where f_0 is the spatial fringe frequency and □ *(r)* is the phase containing the wave front slope Δ*w (x, y)* information. The *a(x, y)* and *b(x, y)* define the intensity modulations arising from the imperfections in the polarizer and analyzer and the birefringent material transmission or reflection. The local phase information in the interferogram relates to the local wave front slope as defined by the equation (10).

Using one-dimensional Fourier Transform, Takeda et al[11] have suggested a method for interferogram analysis. The same has been extended to two-dimensional Fourier transform by Roddier[12], Macy[13] and Bone et. al.[14]). Same approach has been adopted for present interferogram analysis and wavefront retrieved.
The intensity function can be written in the complex form as follows.

$$I(x,y) = a(x,y) + \frac{1}{2}b(x,y)\begin{bmatrix}\cos\{2\pi f_o.x + \phi(x,y)\} + i\sin\{2\pi f_o.x + \phi(x,y)\} \\ +\cos\{2\pi f_o.x + \phi(x,y)\} - i\sin\{2\pi f_o.x + \phi(x,y)\}\end{bmatrix} \qquad (11)$$

This equation can be written in more convenient form as

$$I(x,y) = a(x,y) + \frac{1}{2}b(x,y)\left\{e^{i\phi(x,y)}e^{i2\pi f_o x} + e^{-i\phi(x,y)}e^{-i2\pi f_o x}\right\} \qquad (12)$$

Let $c(x,y) = \frac{1}{2}b(x,y)e^{i\phi(x,y)}$ and $c^*(x,y)$ its complex conjugate. Then equation (12) becomes

$$I(x,y) = a(x,y) + c(x,y)e^{i2\pi f_o x} + c^* e^{-i2\pi f_o x} \qquad (13)$$

Applying the Fast Fourier Transform (FFT) on the intensity distribution, it becomes

$$\hat{\boldsymbol{I}}(f,y) = \hat{\boldsymbol{A}}(f,y) + \boldsymbol{C}(f - f_o, y)\,\boldsymbol{C}^*(f + f_o, y) \qquad (14)$$

Where $\hat{\boldsymbol{I}}$ denotes the Fourier transform of intensity distribution, $\boldsymbol{A}$ is the Fourier transform the function a(x, y), $\boldsymbol{C}$ is the Fourier transform of the function c(x, y) and f is the spatial frequency in the x-direction. By knowing the spatial carrier frequency of f_o apriori, by the method described earlier, choose either of the spectra say, $\boldsymbol{C}(f - f_o, y)$ and translate it by +/- f_o on the frequency axis toward the origin to get $\boldsymbol{C}(f, y)$. The unwanted low frequency modulation and the high frequency noise have been filtered out at this stage. Setting zero the other frequencies and shifting the result by an amount f_o to

eliminate the carrier frequency. Again using inverse Fourier transform of ***C(f, y)*** with respect to f obtain c(x, y) as defined in the equation.

In other words

$$c(x,y) = \frac{1}{2} b(x,y) e^{i\phi(x,y)} = \frac{1}{2} b(x,y)\cos\phi(x,y) + i\frac{1}{2} b(x,y)\sin\phi(x,y) \quad (15)$$

Therefore, the Phase distribution □ *(x, y)* is given by

□ *(x, y)* = arc tan Imaginary part of *c (x, y)* / Real part of c *(x, y)* = $a\tan\left[\frac{\mathrm{Im}\{c(x,y)\}}{\mathrm{Re}\{c(x,y)\}}\right]$

The Phase so obtained range from –π to +π and the ambiguity is corrected appropriately by suitable phase unwrapping.

V. PHASE UNWRAPPING

Since the arc tangent is a periodic function, □ *(r)* is determined to within a multiple of π. The common aspect of interferogram analysis leads to the necessity of phase unwrapping to remove the ambiguity caused by this loss of information and to recreate a continuous wave front slope. The process of unwrapping the phase to obtain the true phase is the most complicated part of fringe analysis. The algorithm adopted in this case is similar to the analysis described by Bone[14]. The algorithm detects discontinuities of magnitude 2π in every chosen path in the image of the wrapped phase. The algorithm developed using LabVIEW then adds or subtracts Q values of 2π to each point of discontinuity.

VI. WAVE FRONT RECONSTRUCTION

The unwrapped phase produces an array of wave front slope vector that must be reconstructed to retrieve the complete two-dimensional wave front. As mentioned above, the wave front slope is expressed as

$$\Delta W(x,y) = \frac{\partial w}{\partial x} S + \frac{\partial w}{\partial y} T \quad \text{assuming } S \text{ or } T << 1 \quad (16)$$

A direct method of retrieving the wave front is to use the derivations of the Zernike polynomials expressed as a linear combination of Zernike polynomials (Noll 1976). By inserting the Zernike polynomials into the above equations and combining the like terms in the x-derivative and y-derivative and re arrange the resulting expressions as a linear combination of Zernike Polynomials. For M data points, M equations are obtained which are much greater than N-1 Zernike co-efficients. Several authors[4,15] have discussed the standard method of solving such a set of over determined linear equation.

In the matrix notation it can be expressed as

$$\mathbf{W} = \mathbf{A} \,.\, \mathbf{F} \quad (17)$$

where **W** is the wave front slope values, **A** is the N-1 co-efficients of the Zernike to be determined and **F** is the derivatives of the Zernike polynomials for each data point. To solve this equation the inversion of **F** has to be estimated. Matrix **F** is neither square nor singular and the inversion operation becomes very complex. This over determined system is most commonly solved by a least square approach; i.e.,

$$\mathbf{W.F^{-1} = A.F.F^{-1}} \quad (18)$$

$$\mathbf{A = (F^T F)^{-1}.F^T.W} \quad (19)$$

$\mathbf{F^T}$ is the transpose of **F**. Determining the coefficients **A** the wavefront is reconstructed using the Zernike polynomials. Following the above approach a complete data reduction software has been developed using Lab-View version 2010.

VII. EXPERIMENTAL VERIFICATION AND RESULTS

The following are the results of the simulation based on the interferometric theory. The computer simulated interferogram is given in Fig.1. The shear values decides the sensitivity of the method. The phase map (wavefront slope) from PSI method is shown in Fig.2 The contour map of the wave front surface as measured from the PSI is shown in Fig.3.

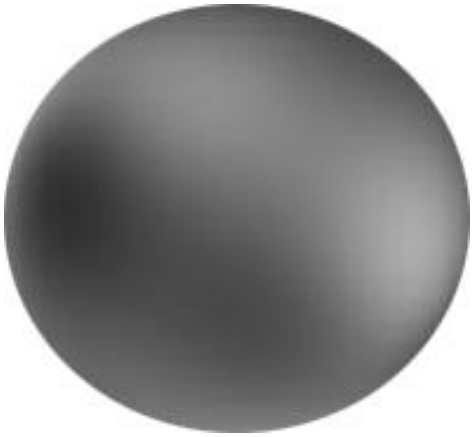

Fig.2. The Phase Map from PSI

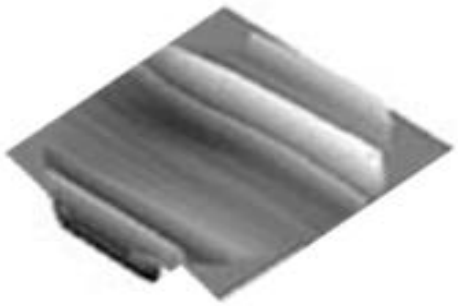

Fig.3. The Surface map of the pupil plane obtained from PSI

The rms and the PV values are expressed in waves. The table compares RMS value computed from the three methods namely the PSI method, OPD interferometric method and the Shack Hartmann sensor. The PSI technique and the Interferometric methods agree well while the SH method gives slightly low value due to poor spatial sampling.

Table 1. RMS Comparision of Different Methods

Method	RMS
PSI Method	0.48
OPD method	0.43
Shack Hartmann	0.38

VIII. CONCLUSION

We have demonstrated the use of Polarization shearing interferometer as a two dimensional shearing wave front sensing device. The convenience of the size, stability with respect to thermal and mechanical disturbances, and insensitivity to vibrations, large dynamic range and capability of high spatial frequency sampling make this device as a best suited wavefront sensing device for adaptive optics application.

REFERENCES

1. J.W.Hardy and A.J.MacGovern, "Shearing Interferometry: a flexible technique for Wavefront measurement," SPIE 816, 180 – 195, (1987).
2. J.W.Hardy, J.E.Lefebvre and C.L.Koliopoulous, "Realtime atmospheric compensation." J.Opt.Soc.Am. 67, 360-369 (1977).
3. J.W.Hardy, "Adaptive Optics: a new technology for the control of light," Proc.IEEE 66, 651-697 (1978).
4. C.M.Humphries, J.W.Harris and E.Atad, "Determination of the Wavefront errors of an astronomical telescope using lateral shearing interferometry," MNRAS, 284,655-668 (1997).
5. D.Malacara, Optical Shop Testing, 2nd Edn. John Wiley & Sons , Inc.
6. A.K.Saxena, "Quantitative Test for concave aspheric surfaces using a Babinet Compensator," Appl.Opt. 18, 2897 (1979).
7. A.K.Saxena and A.P.Jayarajan, "Testing concave aspheric surfaces: Use of two crossed Babinet Compensators", Appl.Opt. 20, 724 (1980).
8. A.K.Saxena and J.P.Lancelot, "Theoretical fringe profiles with crossed Babinet compensators in testing concave aspheric surfaces," Appl.Opt. 21, 4030-4032 (1982).
9. A.K.Saxena and J.P.Lancelot, "Wavefront sensing and evaluation using two crossed Babinet compensators," SPIE, 1121, 41-43 (1990).
10. R.J.Noll, "Zernike Polynomials and atmospheric turbulence" J.Opt.Soc.Am., 66, 207-211 (1976).
11. M.Takeda, H. Ina and S.Kobayashi, "Fourier Transform method of fringe-pattern analysis for computer based tomography and interferometry." J.Opt.Soc. Am, 72, 156-160 (1982).
12. C.Roddier and F.Roddier, "Interferogram analysis using Fourier Transform techniques," Appl.Opt. 26, 1668-1673 (1987).
13. W.W.Macy, Jr., "Two-Dimensional fringe pattern analysis," Appl.Opt. 22, 3898-3901 (1983).
14. D.J.Bone, H.A.Bachor and R.J.Sandeman, "Fringe pattern analysis using a 2-D Fourier Transform," Appl.Opt. 25, 1653-1660 (1986).
15. J.Primot, G.Rousset and J.C.Fontanella, "Deconvolution from wave-front sensing: a new technique for compensating turbulence-degraded images", J.Opt.Soc.Am. A, 7, No.9, 1598-1608 (1990).

